Numerical Study of Interaction between Waves and Floating Body by MPS Method

Y.L. Zhang[1,2], Z.Y. Tang[1,2], D.C. Wan[1,2]*

1. State Key Laboratory of Ocean Engineering, School of Naval Architecture, Ocean and Civil Engineering, Shanghai Jiao Tong University, 2. Collaborative Innovation Center for Advanced Ship and Deep-Sea Exploration, Shanghai 200240, China

*Corresponding author: dcwan@sjtu.edu.cn

Abstract

In the present study, interaction between regular waves and free roll motion of a 2D floating body is investigated by our in-house particle solver MLParticle-SJTU based on modified Moving Particle Semi-Implicit (MPS) method. Numerical wave tank is developed to calculate the interaction between waves and floating body, including wave-maker module and free roll motion module. The comparison between the numerical wave elevation and analytical solution shows that the MLParticle-SJTU can provide acceptable accuracy of wave making. Roll motion and force acting on the floating body in waves are in good agreement with experimental results. Profiles of the wave surface surrounding floating body are presented.

Keywords: Particle method; MPS (Moving Particle Semi-Implicit); Wave Floating body Interaction; Wave making; Roll motion

Introduction

Recent years, a variety of floating structures, such as ships, offshore platforms, floating-breakwater, fish-farms, floating-airports, play a crucial role in coastal and ocean engineering. It's common for floating structures to suffer from loadings under waves, and responses of these structures mounted in ocean or coastal environments have significant relation to the wave impacts. The interaction between free-surface waves and floating body is one of the key aspects in ship design or offshore structure design to increase performance and efficiency.

In the past decades, both theory and experimental analyses methods have been used by many researchers to investigate the interaction problem. The early established theoretical methods are mainly based on potential flow theories and limited to solve the motion of floating body with simple shape. Chahine, et al. (1999) developed a free surface hydrodynamics code based on three-dimensional Boundary Element Method and then they modeled the nonlinear evolution of waves as they progress along a shallow sloping bottom in the presence of a floating body that is free to rotate and translate. Bai and Eatock Taylor (2006) studied the radiation and diffraction problem of vertical circular cylinders in a fully nonlinear numerical wave tank based on the boundary element method (BEM). You and Faltinsen (2012) developed a 3D fully nonlinear time-domain Rankine source code. A numerical wave tank with a piston wave maker and a numerical damping zone is applied to simulate the interaction between moored floating bodies and waves. Jung et al. (2004a) experimentally studied waves impacting on a fixed rectangular structure. PIV technique is used to obtain the mean velocity and turbulence properties of water around structure. The generation and evolution of vortexes of a barge in beam sea condition is simulated. Subsequently, Jung et al. (2004b, 2005) investigated the two-dimensional flow characteristics of interactions between waves

and freely rolling rectangular structures. Results between the roll motion and the fixed condition were compared. Ren et al. (2015) studied the motions of a freely floating body under nonlinear waves.

Besides, a wide variety of nonlinear numerical models based on the NS equations in time domain have been developed to study the interaction problem. The finite difference method or the finite volume method (FVM) is typically used for spatial discretization. And various techniques are used for interface capturing, such as the Level Set method and the Volume of Fluid method. In Boo's work (2002), a numerical tank was constructed, the linear and nonlinear irregular wave diffraction forces acting on a submerged structure was predicted. In Li's work (2010), a 2-D numerical regular wave tank was built, which mainly based on the spatially averaged Navier- Stokes equations and the k-e model was used to simulate the turbulence of flow. The fully nonlinear wave-body interactions between a surface piercing body in finite water depth and flat/slop bottom topography were also investigated. Ye et al. (2012) constructed a three-dimensional numerical wave tank with a newly developed solver naoe-FOAM-SJTU based on the open source code library OpenFOAM, and a S-175 container ship sailing in regular heading waves was simulated. Zha, et al. (2013) studied the motion responses of heave and pitch of a ship in different wave conditions. Numerically simulation of the motion response of a moored floating pier in regular waves was described in Liu and Wan (2013).

The above researches are based on Eulerian methods and grids are necessary for spatial discretization. It's difficult and inaccurate to obtain free surface with large deformation. Recently, Lagrangian particle methods draw much attention of researchers and are seen as promising numerical approaches for free surface flows. For example, Moving Particle Semi-implicit (MPS), originally proposed by Koshizuka and Oka (1996) for incompressible flow. In the present study, a particle solver, MLParticle-SJTU based on modified Moving Particle Semi-Implicit (MPS) method, is used for all simulation works. Some improved schemes are used in this solver to suppress numerical unphysical pressure oscillation usually observed in traditional MPS method. These improvements include: (1) momentum conservative pressure gradient model; (2) modified kernel function [Zhang et al., 2011b]; (3) mixed sourced term method for Poisson equation of pressure [Tanaka et al., 2010]; (4) surface detection method based on asymmetry of neighbor particles [Zhang et al., 2011a]. The MLParticle-SJTU was applied in many large free-surface deformation problems, such as dam breaking flow [Zhang, et al., (2011c, 2014)], liquid sloshing in LNG tank [Zhang, et al., 2012; YANG, et al.,2014], Floating Body Interacting with Solitary Wave [Zhang, et al., 2011b].

This paper is organized as follow: Firstly, the MPS method for incompressible fluid is described. Numerical approach to solve the motion of floating body is introduced. Then, numerical wave tank is developed to calculate the interaction between waves and floating body, including wave-maker module and free roll motion module. Time history of wave propagation is measured and compared with the analytical solution to validate the accuracy of wave making. At last, roll motion and force acting on the floating body in waves is calculated and compared with experimental results. Profiles of the wave surface surrounding floating body are also presented.

Numerical Scheme

Governing Equations

Governing equations are the continuum equation and the momentum equation. These equations for incompressible viscous fluid are represented as：

$$\nabla \cdot \boldsymbol{V} = 0 \tag{1}$$

$$\frac{D\boldsymbol{V}}{Dt} = -\frac{1}{\rho}\nabla P + \nu\nabla^2 \boldsymbol{V} + \boldsymbol{g} \tag{2}$$

where $\boldsymbol{V}$ is the velocity vector，t is the time, ρ is the density，P is the pressure，v is the kinematic viscosity, g is the gravity acceleration.

Particle Interaction Models

Kernel Function

In particle method, governing equations are transformed to the equations of particle interactions. The particle interactions are based on the kernel function. In traditional MPS method, the kernel function is expressed as follow (Koshizuka, 1996):

$$W(r) = \begin{cases} \dfrac{r_e}{r} - 1 & 0 \le r < r_e \\ 0 & r_e \le r \end{cases} \tag{3}$$

A drawback of the above kernel function is that it becomes singular at r=0. This may cause unreal pressure between two neighboring particles with a small distance, and affect the computational stability. To overcome this, an improved kernel function is used in this paper (Zhang and Wan, 2011b):

$$W(r) = \begin{cases} \dfrac{r_e}{0.85r + 0.15r_e} - 1 & 0 \le r < r_e \\ 0 & r_e \le r \end{cases} \tag{4}$$

The above kernel function has a similar form with the original kernel function Eq. (3), but without singularity.

Gradient Model

Gradient operator is modeled as a local weighted average of the gradient vectors between particle i and its neighboring particles j:

$$< \nabla\phi >_i = \frac{D}{n^0} \sum_{j \ne i} \frac{\phi_j + \phi_i}{|\boldsymbol{r}_j - \boldsymbol{r}_i|^2} (\boldsymbol{r}_j - \boldsymbol{r}_i) \cdot W(|\boldsymbol{r}_j - \boldsymbol{r}_i|) \tag{5}$$

where ϕ is an arbitrary scalar function, D is the number of space dimensions, n^0 is the initial particle number density for incompressible flow. The particle number density in MPS method is defined as:

$$< n >_i = \sum_{j \ne i} W(|\boldsymbol{r}_j - \boldsymbol{r}_i|) \tag{6}$$

Laplacian Model

Laplacian operator is derived by Koshizuka et al. (1998) from the physical concept of diffusion as：

$$< \nabla^2\phi >_i = \frac{2D}{n^0\lambda} \sum_{j \ne i} (\phi_j - \phi_i) \cdot W(|\boldsymbol{r}_j - \boldsymbol{r}_i|) \tag{7}$$

$$\lambda = \frac{\sum_{j \ne i} W(|\boldsymbol{r}_j - \boldsymbol{r}_i|) \cdot |\boldsymbol{r}_j - \boldsymbol{r}_i|^2}{\sum_{j \ne i} W(|\boldsymbol{r}_j - \boldsymbol{r}_i|)} \tag{8}$$

where λ is a parameter, introduced to keep the variance increase equal to that of the analytical solution. Both viscous force $\nabla^2 \boldsymbol{V}$ in Eq. (2) and $\nabla^2 P$ in the right hand side of the PPE (Eq. 9 and Eq. 10) are discretized by Eq. (7).

Model of incompressibility

The incompressible condition in traditional MPS method is represented by keeping the particle number density constant. In each time step, there are two stages: first, temporal velocity of particles is calculated based on viscous and gravitational forces, and particles are moved according to the temporal velocity; second, pressure is implicitly calculated by solving a Poisson equation, and the velocity and position of particles are updated according to the obtained pressure.

The pressure Poisson equation in traditional MPS method is defined as (Koshizuka et al., 1998):

$$< \nabla^2 P^{k+1} >_i = -\frac{\rho}{\Delta t^2} \frac{< n^* >_i - n^0}{n^0} \tag{9}$$

where $n*$ is the particle number density in temporal field.

The source term of the Poisson equation in Eq. (9) is solely based on the deviation of the temporal particle number density from the initial value. As the particle number density field is not smooth, the pressure obtained from Eq. (9) is prone to oscillate in spatial and temporal domain. To suppress such unphysical oscillation of pressure, Tanaka and Masunaga (2010) proposed a mixed source term for PPE, which combines the velocity divergence and the particle number density. The main part of the mixed source term is the velocity divergence, while the particle number density is used to keep the fluid volume constant. This improved PPE is rewritten by Lee et al. (2011) as:

$$< \nabla^2 P^{k+1} >_i = (1-\gamma) \frac{\rho}{\Delta t} \nabla \cdot V_i^* - \gamma \frac{\rho}{\Delta t^2} \frac{< n^k >_i - n^0}{n^0} \tag{10}$$

where γ is a blending parameter with a value between 0 and 1. The value of γ has large effect on the pressure field. In particular, the larger γ produces smoother pressure field. However, the volume of fluid cannot be constant while $\gamma = 0$. The effects of γ have been investigated by Tanaka, et al. (2010) and Lee, et al. (2011). $\gamma = 0.01$ is used in this paper.

Free Surface boundary condition

On the surface particles, the free surface boundary conditions, including kinematic and dynamic boundary condition, are imposed. The kinematic condition is directly satisfied in Lagrangian particle method, while the dynamic condition is implemented by setting zero pressure on the free surface particles. So the accuracy of surface particle detection has significant effect on pressure field.

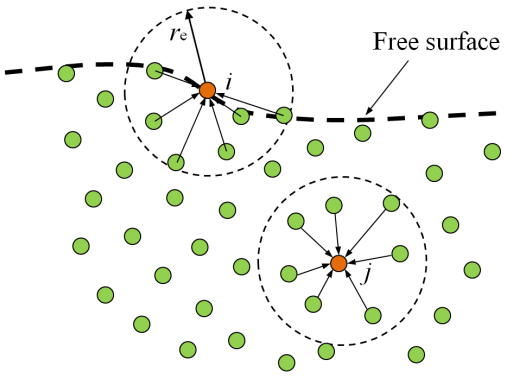

Figure 1. Description of particle interaction domain

The interaction domain is truncated in the free surface (Fig. 1), so the particle number density near the free surface is lower than that in the inner field. In traditional MPS method, particle satisfying (Koshizuka et al., 1998):

$$< n >_i^* \ < \ \beta \cdot n^0 \tag{11}$$

is considered as free surface particle, where β is a parameter, can be chosen between 0.80 and 0.99.

The traditional detection method (Eq. 11) is based on the particle number density. However, inner particles with small particle number density may be misjudged as free surface particles, thus unreal pressure around the misjudged particles occur. This usually causes nonphysical pressure oscillation. To improve the accuracy of surface particle detection, we employ a new detection method in which a vector function is defined as follow (Zhang and Wan, 2011c):

$$< \boldsymbol{F} >_i = \frac{D}{n^0} \sum_{j \neq i} \frac{1}{| \boldsymbol{r}_i - \boldsymbol{r}_j |} (\boldsymbol{r}_i - \boldsymbol{r}_j) W(\boldsymbol{r}_{ij}) \tag{12}$$

The vector function $\boldsymbol{F}$ represents the asymmetry of arrangements of neighbor particles.

Particle satisfying:

$$<| \boldsymbol{F} |>_i \ > \ \alpha \tag{13}$$

is considered as free surface particle, where α is a parameter, and has a value of 0.9 $|\boldsymbol{F}|^0$ in this paper, $|\boldsymbol{F}|^0$ is the initial value of $|\boldsymbol{F}|$ for surface particle.

It should be specially noted that the Eq. (13) is only valid for particles with number density between $0.8n^0$ and $0.97n^0$ since particles with number density lower than $0.8n^0$ is definitely surface particles, while those with number density higher than $0.97n^0$ should get pressure through Poisson equation.

Motion of floating body

The motion of the floating body is governed by the equations of rigid body dynamics, following the Newton's law of motion. The translation motion of the center of gravity and the rotation of the rigid body are given in a simple 2-D framework by

$$\begin{cases} M \dfrac{d\boldsymbol{V}_G}{dt} = M\boldsymbol{g} + \boldsymbol{F}_{fluid-solid} \\ I_G \dfrac{d\boldsymbol{\Omega}_G}{dt} = \boldsymbol{T}_{fluid-solid} \end{cases} \tag{14}$$

where M and I_G are the mass and the moment of inertia of the floating body around the center of gravity, respectively. $\boldsymbol{V}_G$ and $\boldsymbol{\Omega}_G$ are the linear velocity of the center of gravity and the angular velocity of the body, respectively. $\boldsymbol{F}_{fluid-solid}$ is the hydrodynamic force acting on the body, $\boldsymbol{T}_{fluid-solid}$ is the hydrodynamic torque with the direction normal to the plane.

Numerical Simulations

Test of wave making

In present work, a piston-type wave generator was incorporated in the left side of 2D numerical wave tank. A slop beach was installed at the end of the wave tank to absorb waves and avoid reflection. Sketch of the numerical setup is shown in Fig. 2. The numerical wave tank is 5.5 m

width and 1.5 m height with initial water depth 0.9 m. Wave conditions used in present numerical test is shown in Table 1, and travelling waves were generated based on linear wave theory.

Table1. Parameters of wave making

Parameters	Values
Water density	1000(kg/m^3)
Water height	0.9(m)
Wave length	1(m)
Wave height	0.029
Wave period	0.8(s)
Fluid spacing	0.004 (m)
No. of fluid particles	132750
No. of total particles	138130

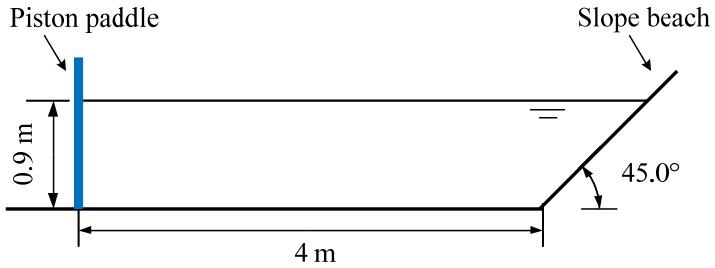

Figure 2. Sketch of the 2-D wave tank

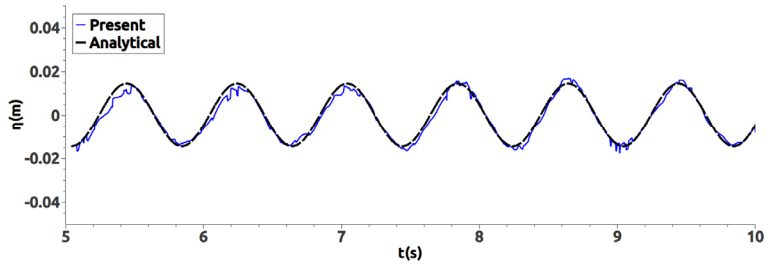

Figure 3. Comparison between numerical wave elevation and analytical solution at location 1m from the piston paddle

Fig. 3 shows a comparison between numerical wave elevation and analytical solution at the location 1 m from the initial position of piston paddle. The trend of numerical free surface height is in agreement with analytical solution except that the former is less smoother than the later. The difference can be improved by reducing the particle space.

Simulation of freely rolling body

In this section, the roll motion of a 2D floating rectangular structure in a numerical wave tank was investigated in time domain. The wave generator and wave absorbing manner here are same as that in previous section. The width and height of the rectangular floating body are 0.3 m and 0.1 m, respectively. The structure was installed at the point 1.2 m from the wave maker and 0.9 m above the bottom of tank, fixed at the center of its gravity but free in the degree of roll. The initial geometry and set-up are shown in Fig. 4.

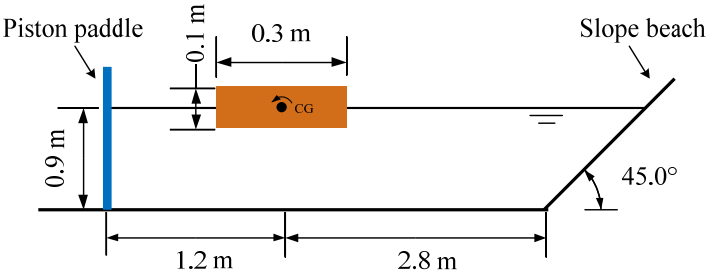

Figure 4. Sketch of the freely rolling body

In present simulation, the distance between particles is 0.004 m, the total number of particles is 137718 while the number of fluid particles is 131762. The gravitational acceleration and water density are 9.8m/s^2 and 1000kg/m^3. The kinematic viscosity of water is given by 1.01×10^{-6} m^2/s. The time step size is 0.0004s and the total computational time is 10s.Waves with period of 0.8 s, was generated in the present study. The wave conditions used in present computation are same as shown in Table 1.

In the free rolling test of rectangular structure, angles of roll motion about the center of gravity were measured when the regular roll motion of rectangular body can be obtained.

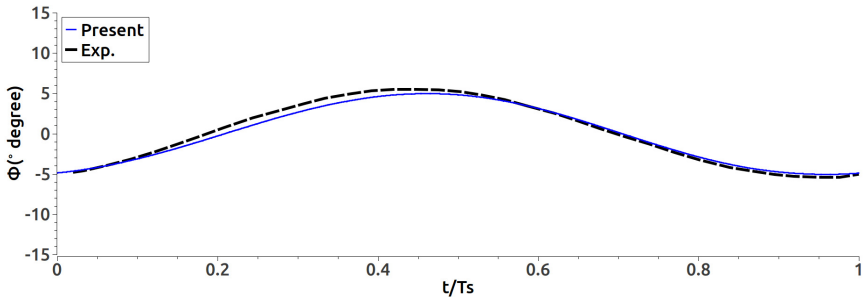

Figure 5. Rolling motion of the rectangular body within wave period (solid line: result of simulation; dashed line: result of JUNG)

Fig. 5 shows the inclined angle of the rectangular structure over one period of the regular wave. Results about the roll motion of floating body is compared between present simulation and experiment by Jung(2004). It can be found that both the pattern of curves and amplitude of roll angles are in good agreement.

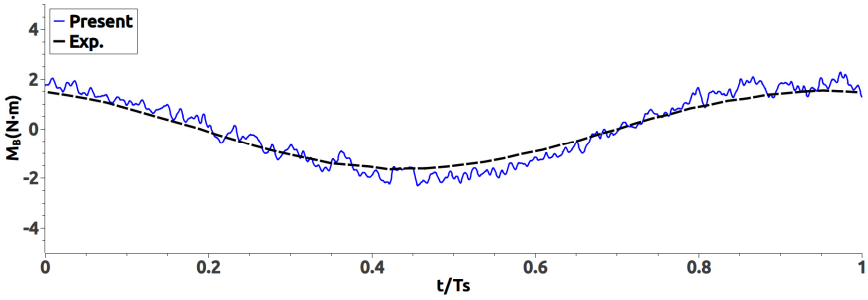

Figure 6. Time history of buoyancy restoring moment of the rectangular body within wave period (solid line: result of simulation; dashed line: result of JUNG)

Details about buoyancy restoring moment (M_B) of the freely rolling body should be noteworthy, because the roll motion is closely related with the change of M_B in time domain. Fig. 6 shows the time history of buoyancy restoring moment in one wave period. It can be seen that the calculated

results of M_B agree fairly well with experimental results, though the calculated curve about moment has a little nonphysical fluctuations.

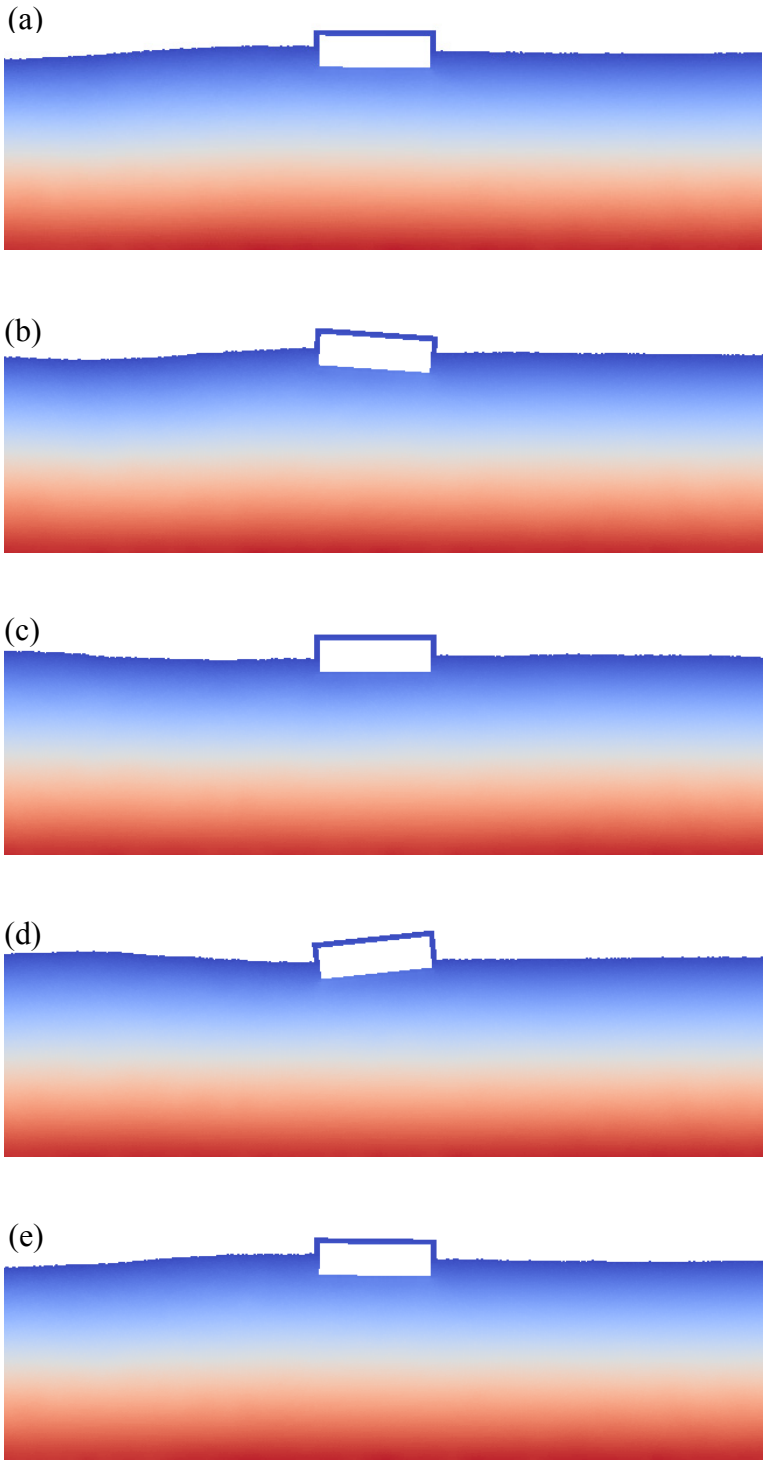

Figure 7. Rotary positions and wave surfaces around floating box, (a) t=t0, (b) t=t0+T/4, (c) t=t0+T/2, (d) t=t0+3T/4, (e) t=t0+T

Fig. 7 shows the evolution process of rotation of the floating body. It can be seen that positions of the floating box is strong influenced by the propagation of incident wave through five snapshots of representative-instants (t0, t0+T/4, t0+T/2, t0+3T/4 and t0+T) in a wave period. Firstly, the body rotates clockwise until the value of M_B climbs up to the maximum with the coming wave from left.

After that, the crest of the wave transfers from left to right of the floating box. At the same time, buoyancy restoring moment of the body decreases. As a result, box rotates anti-clockwise and returns to horizontality at the instant of t0+T/2. With the propagating of the wave, water surface falling on the left and rising on the right from t0+T/2 to t0+3T/4. Box keeps on rotating anti-clockwise until the value of M_B declines to the minimum. Form the instant of t0+3T/4, it begins to rotate clockwise again, and returns to nearly horizontality at t0+T finally. The rotation of floating body will repeat with the next coming wave from left.

Conclusions

In this paper, interaction between regular waves and free roll motion of a 2D floating body is investigated by our in-house particle solver MLParticle-SJTU based on modified Moving Particle Semi-Implicit (MPS) method. Four improvements, including nonsingular kernel function, momentum conservative pressure gradient model, mixed source term for PPE and an accurate surface detection method, are employed in this solver. Numerical wave tank is developed to calculate the interaction between waves and floating body, including wave-maker module and free roll motion module. The comparison between the numerical wave elevation and analytical solution shows that the MLParticle-SJTU can provide acceptable accuracy of wave making. Numerical roll motion and force acting on the floating body in waves are in good agreement with experimental results. At last, the evolution process of rotation of the floating body was shown through five snapshots of representative-instants (t0, t0+T/4, t0+T/2, t0+3T/4 and t0+T) in a wave period. It can be seen that positions of the floating box are strong influenced by the propagation of incident wave. According to the results present in previous sections, the solver can be used to deal with waves floating body interaction problems.

Acknowledgement

This work is supported by National Natural Science Foundation of China (Grant Nos. 51379125, 51490675, 11432009, 51411130131), The National Key Basic Research Development Plan (973 Plan) Project of China (Grant No. 2013CB036103), High Technology of Marine Research Project of The Ministry of Industry and Information Technology of China, Chang Jiang Scholars Program (Grant No. T2014099) and the Program for Professor of Special Appointment (Eastern Scholar) at Shanghai Institutions of Higher Learning (Grant No. 2013022), to which the authors are most grateful.

References

Bai, W., and Taylor, R. E. (2008) Fully nonlinear simulation of wave interaction with fixed and floating flared structures, *Ocean Engineering*, 36(3), 223-236.

Boo, S.Y., (2002) Linear and nonlinear irregular waves and forces in a numerical wave tank, *Ocean Engineering*, 29, 475-493.

Jung, K.H., Chang, K.A. and Huang, E.T. (2004a) Two-dimensional flow characteristics of wave interactions with a fixed rectangular structure. *Ocean Engineering*, 31, 975-998.

Jung, K. H. (2004b) Experimental study on rectangular barge in beam sea, Ph.D. Texas A&M University.

Jung, K.H., Chang, K.A. and Huang, E.T. (2005) Two-dimensional flow characteristics of wave interactions with a free-rolling rectangular structure. *Ocean Engineering*, 32(1), 1-20.

Kalumuck, K. M., Chahine, G. L., and Goumilevski, A. G. (1999) *BEM modeling of the interaction between breaking waves and a floating body in the surf zone*, 13th ASCE Engineering Mechanics, Baltimore, Maryland.

Koshizuka, S., and Oka, Y. (1996) Moving-particle Semi-implicit Method for Fragmentation of Incompressible Fluid, *Nuclear Science and Engineering*, 123, 421-434.

Koshizuka, S., Obe, A., and Oka, Y. (1998) Numerical Analysis of Breaking Waves Using the Moving Particle Semi-implicit Method, *International Journal for Numerical Methods in Fluids*, 26, 751-769.

Li, Y., and Lin, M. (2010) Wave-body interactions for a surface-piercing body in water of finite depth, *Journal of hydrodynamics, Ser. B*, 22 (6), 745-752.

Liu, Y. C., and Wan, D. C. (2013) *Calculation of motion response for moored floating pier in waves*, Proc 25rd Chinese National Conf Hydrodynamics, ZhouShan, China.
Ren, B., He, M., Dong, P., and Wen, H. j. (2015) Nonlinear simulations of wave-induced motions of a freely floating body using WCSPH method, *Applied Ocean Research*, 50 (2015) 1-12.
Tanaka, M., and Masunaga, T. (2010) Stabilization and smoothing of pressure in MPS method by Quasi-Compressibility, *J Comp Phys*, 229, 4279-4290.
YANG Y. Q., ZHANG Y. X., Tang Z. Y., and WAN D. C. (2014) *Numerical study on liquid sloshing in horizontal baffled tank by MPS method*, Proc 26rd Chinese National Conf Hydrodynamics, QingDao, China.
You, J., Faltinsen, and O. M. (2012) *A 3D Fully Nonlinear Numerical Wave Tank with a Moored Floating Body in Shallow Water*, Proceedings of the Twenty-second International Offshore and Polar Engineering Conference Rhodes, Greece.
Ye, H. X., Shen, Z. R., and Wan, D. C. (2012) *Numerical analysis of large amplitude motion responses for a container ship in waves*, Proc 24rd Chinese National Conf Hydrodynamics, Wuxi, China.
Zha, R, S, Ye, H. X., and Wan, D. C. (2013) *Numerical investigation of ship sea-keeping performances in head regular waves*, Proc 25rd Chinese National Conf Hydrodynamics, ZhouShan, China.
Zhang, Y. X., and Wan, D. C. (2011a) *Application of Improved MPS Method in Sloshing Problem*, Proc 23rd Chinese National Conf Hydrodynamics, Xi'an, China.
Zhang, Y. X., and Wan, D. C. (2011b) *Apply MPS Method to Simulate Motion of Floating Body Interacting with Solitary Wave*, Proc 7th Int Workshop Ship Hydrodynamics, IWSH, Shanghai, China, 275-279.
Zhang, Y. X., and Wan, D. C. (2011c) Application of MPS in 3D Dam Breaking Flows, *Sci Sin Phys Mech Astron*, 41, 140-154.
Zhang, Y. X., and Wan, D. C. (2012) *Apply MPS Method to Simulate Liquid Sloshing in LNG Tank*, Proc 22nd Int Offshore and Polar Eng Conf, Rhodes, Greece, 381-391.
Zhang, Y. X., Wan, D. C., Hino, and Takanori. (2014) Comparative study of MPS method and level-set method for sloshing flows, *Journal of hydrodynamics*, 26(4), 577-585.
Zhang, Y. X., TANG, Z. Y., and Wan, D. C. (2013) *Simulation of 3D dam break flow by parallel MPS method*, Proc 25rd Chinese National Conf Hydrodynamics, ZhouShan, China.